Robotica (2013) volume 31, pp. 837–851. © Cambridge University Press 2013
doi:10.1017/S0263574713000039

Application of phase-plane method in generating minimum time solution for stable walking of biped robot with specified pattern of motion

Mohammad Jafar Sadigh* and Saeed Mansouri

Department of Mechanical Engineering, Isfahan University of Technology, Isfahan, Iran

(Accepted January 8, 2013. First published online: February 21, 2013)

SUMMARY

Walking with a maximum speed is an interesting subject in the field of biped motion. Giving an answer to the question of "what is the maximum achievable speed of a certain biped walking with a physically acceptable pattern?" is the main objective of this work. In this paper, minimum time motion of biped was studied during one step that consists of single support phase (SSP) and double support phase (DSP). The minimum time problem is formulated with stability and non-slip conditions along with actuator limits expressed as some inequality constraints. In addition, certain kinematic constraints in terms of hip joint position are considered that ensure an acceptable walking pattern. A phase-plane technique is used to find the minimum time solution. A numerical simulation is given to shed some light on how the proposed method works. Validity and effectiveness of the method are verified by comparing the results with those of other researches.

KEYWORDS: Minimum time motion; Bipeds; Stability and non-slip condition; Phase-plane analysis.

1. Introduction

Locomotion of biped robots has gained lots of attention during the past few decades. While stability was initially the main issue of research, optimization and improving the pattern of motion are now the most important issues studied by researchers.

Vukobratovic *et al.*[1,2] proposed a stability criterion known as zero moment point (ZMP) that guarantees walking stability. They defined ZMP as a point on the ground where moment of all gravitational and inertial forces acting on the robot is zero about two axes lying in the plane of the ground. A sufficient condition for stability was stated to keep this point within the supporting polygon during motion. This method was employed by many researchers to plan stable walking gait for bipeds. Kajita *et al.*,[3,4] Park and Kim,[5] and Erbatur and Kurt[6] used a linear model of inverted pendulum in path planning for a stable motion of biped. However, due to approximations in the dynamic model, ZMP did not exactly track the desired trajectory. Takanishi *et al.*[7] and Yamaguchi *et al.*[8] considered a dynamic model of the biped. They used Fourier series functions for hip joint and track to design the motion such that ZMP follows a prescribed trajectory. However, it was difficult to determine the desired ZMP trajectory to have appropriate performance. To deal with this problem, Huang *et al.*[9] proposed a method of gait synthesis without first prescribing the desired ZMP trajectory. In this method, foot and hip trajectories are planned beforehand in Cartesian space using cubic spline interpolation. They formulated the smooth hip motion using two parameters and computed them to obtain largest stability margin, by which they mean to keep ZMP trajectory near the center of the stable region.

Besides dealing with motion stability, many researchers tried to optimize the motion. Most attention is paid in this field to minimization of the consumed energy.[10–12] Optimization of actuator demand is another subject studied in refs. [13–16]. Speed of bipeds is another important characteristic that has been improving among different generations of bipeds. Chevallereau and Aoustin[17] obtained optimal cyclic gait for a biped robot without actuated ankle. The gait is composed uniquely of successive single support phase (SSP) and instantaneous impact. They took the joints variables as polynomial functions and then found their coefficients in order to optimize the walking speed and to insure cyclic motion of the biped. Miossec and Aoustin[18] employed a time-optimal control law in double support phase (DSP) to show how such control can improve stability of the walk. In this research, they tried to present a one-dimensional stability analysis based on Poincare map. Dip *et al.*[19] optimized bipedal walking gait by considering the tradeoff between stability margin and speed. They applied a genetic algorithm approach to optimize the key parameters of the walking trajectory and the step length for a certain step period such that stability margin is maximized. Torque limits were not utilized for calculating the optimal speed. In another work Tlalolini *et al.*[20] tried to design a path that could minimize the energy cost of a biped while walking with a desired speed. They, then, tried to increase the walking speed by a search strategy in which the desired speed was increased step by step. One of the main conclusions of this study is that the maximum velocity substantially increases by the introduction of the foot rotation sub-phase in SSP. Although this study could give a systematic approach to increasing the walking speed, it could not give the answer to the maximum achievable speed of the biped. Sadigh and

* Corresponding author. E-mail: jafars@cc.iut.ac.ir

Mansouri[21] arranged a parameter study to find out effect of step length and step period on biped motion. They employed ZMP criteria for stable path planning for several values of step size and step period. They then chose feasible motion among them based on feasibility of actuator limits. This way they found maximum possible speed of the biped for stable walking. Although this parameter study could potentially give a solution to the question of minimum time motion, it could not practically be used due to huge amount of computational effort needed to find the solution.

Essentially, two quite different methods have been developed to generate optimal gait trajectories. The most frequently used approach is based on parametric optimization, whereas the second goes within the framework of optimal control theory. Parametric optimization techniques developed for the purpose of motion optimization mostly rely on representing the motion of biped as functions of time defined by a finite set of discrete parameters to be dealt with as optimization variables. The resulting nonlinear optimization problem can be solved by implementing sequential quadratic programming algorithms, genetic algorithm, etc. Parametric optimization is an efficient means of computing suboptimal trajectories. However, due to the fact that discrete optimization variables are reduced to a finite number, complete fulfillment of constraints, defined over the whole range of time, may be difficult to achieve. In the second method, the optimization problem is considered as an optimal control problem to be dealt with using the Pontryagin maximum principle.

This paper is an effort toward giving a more rigorous solution to the problem of minimum time motion of a specified biped walking stably on a flat surface, while satisfying kinematics constraints of a desired gait such as preventing heel impact with the ground at the end of SSP. One strategy to solve this problem is to minimize the total time necessary for moving a certain distance. To this end, one might minimize the index $J = \int dt$ subject to equality constraints of equations of motion and kinematic constraints, and inequality constraints of actuator limits and stability and non-slip conditions. Although such strategy is suitable for problem formulation, it may not be for obtaining a solution. This approach ends in solving a set of ordinary differential equations with two-point boundary values that are to be solved while considering inequality constraints of stability and non-slip condition. Obtaining a solution to this problem seems to be very difficult due to complexity of the dynamics, its different nature during SSP and DSP, and difficulty of dealing with Coulomb friction during numerical simulation needed in shooting method.

Instead of this strategy an algorithm based on phase-plane analysis was used to obtain the minimum time solution, which was first introduced for serial manipulators by Bobrow *et al*.[22] In this strategy, we tried to find minimum time motion during a complete step with known step length and then to find the best step length that maximizes the walking speed. The minimum time motion is solved for SSP and DSP simultaneously. We introduce an algorithm to find total solution that satisfies initial and final conditions that ensure periodic walking constraint. One should note that although frameworks of the minimum time problem for both SSP and DSP are the same, the constraints are different; moreover, complexity grows in DSP due to closed kinematic configuration of system in this phase.

Phase-plane algorithm for solution of minimum time problem of a non-redundant serial manipulator along specified path subject to actuator limits was first introduced by Bobrow *et al*.[22] They stated that minimum time motion for such system is bang-bang in terms of tangential acceleration of tip of manipulator along the specified path. They also argued that due to actuator limit there would be a speed limit, along the path, beyond which no combination of actuator efforts could keep the manipulator on desired path. Such speed limit divides the phase plane into two feasible and non-feasible regions. Considering the fact that in phase plane the minimum time trajectory is the highest feasible one, they proposed to move the manipulator either with maximum or minimum acceleration along the path in such a way that the solution trajectory never enters non-feasible region. To this end, they used a trial-and-error method to find the switching points such that solution curve in phase plane comes in contact with non-feasible boundary (NFB) without crossing it. While the proposed method was theoretically an important advancement in solution of minimum time motion of manipulators, from a practical point of view it was very difficult and numerically inefficient. Pfeiffer and Johanni[23] improved the method proposed by Bobrow. They introduced the concept of critical points that are candidates of switching points for multi-switch cases. They also proposed an algorithm to construct NFB and to establish switching curve in phase plane for serial manipulators. Zlajpah[24] studied characteristics of solution curve for a manipulator moving on a specified path in phase plane and introduced concept of trapped area and locked area that later on was proved by Ghasemi and Sadigh[25] to be very essential in establishing the switching curve. Verscheure *et al*.[26] presented a general theoretical method to transform the problem of time-optimal path tracking to a convex optimal control problem with a single state. They then presented some convexity-preserving extensions that can be used for other optimal problems.

Moon and Ahmad[27,28] and Bobrow *et al*.[29] extended this method for cooperative non-redundant manipulators. They employed a linear programming approach to find the maximum and minimum acceleration along the path, which needs lots of computation effort. This burden was later on lifted by Sadigh and Ghasemi[30] who proposed to solve a set of linear equations, which takes advantage of pattern of saturated actuators in the previous step, to find maximum and minimum acceleration along the path. Afterwards, they extended the method introduced by Pfeiffer and Johanni[23] for computation of NFB and calculation of maximum and minimum acceleration for parallel manipulators.[31,32]

As explained before, we try to find minimum time solution for stable motion of biped during a complete gait for a specific path in sagittal plane. To find a physical and realizable solution, we need to consider a constrained solution. Stability and slippage prevention are two important constraints that are to be considered. In addition, we also need to consider some kinematic constraints necessary for an acceptable pattern of motion. For instance, a global minimum time solution that

https://doi.org/10.1017/S0263574713000039 Published online by Cambridge University Press

causes foot to hit the ground or a drastic motion for knee or hip joint or even an oscillatory motion for trunk cannot be regarded as an acceptable solution.

To this end, horizontal hip position was considered as the independent parameter of motion and then all other degrees of freedom were related to that by physical kinematic constraints that ensures acceptable pattern of motion. Solving this minimum time problem is equivalent to plan the path for horizontal hip joint that minimizes the time elapse of motion while satisfying all imposed constraints. This basically turns the problem into one similar to what was solved by Bobrow *et al*.[22] and other researchers who followed this method; however, one still faces the following difficulties in using the phase-plane analysis to find the minimum time solution:

(1) The initial and final speeds, which in this technique are supposed to be known, are not known here.
(2) Nature and form of the constraint equations—that plays an important role in calculation of switching points and maximum acceleration and deceleration in phase-plane method—are different from what we are facing in this problem.

To circumvent this problem, we tried to cast the constraints of the problem in a form that can be handled by the phase-plane technique and then introduced the solution algorithm based on that.

Although this paper can be considered as one of the first effort toward the minimum time path planning of a biped in a complete step with SSP and DSP, yet its main contribution can be considered in the way the problem is formulated and casted in a framework that can be solved by a rather straightforward method of phase plane. This method not only is simpler than numerical methods, but it also guarantees to give the solution. The main obstacles in using phase-plane techniques, as mentioned before, were how to express constraints of periodicity of motion, balance stability, and non-slip walking in a framework that can be handled by the phase-plane method.

Mathematical modeling of biped is given in the next section. In the third section, we introduce kinematic constraints of a desired motion. The proposed solution algorithm is introduced in Section 4. Two numerical examples are given in the fifth section to show how the method works. One of these examples is chosen to compare the results obtained in this study with those published by Tlalolini *et al*.[20] that help validate the effectiveness of the proposed method in generating minimum time solution. Concluding remarks of this study are given in the last section.

2. Mathematical Modeling

As stated before, the objective of this study is to find minimum time stable path during one step that consists of SSP and DSP. Such minimum time motion needs to satisfy equations of motion and stability and non-slip condition as constraint equations. In this section, we first develop these equations and then state mathematical form of minimum time problem.

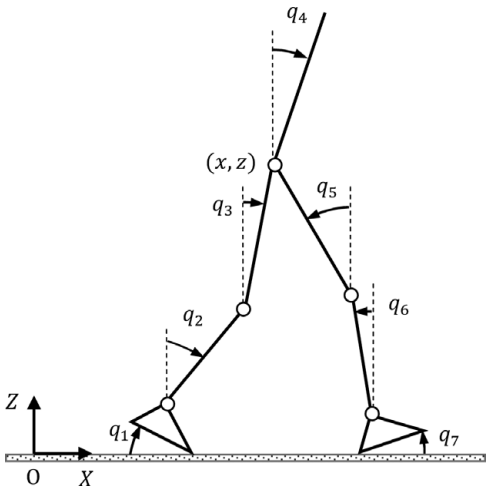

Fig. 1. Seven-link model of a planar biped robot.

2.1. Equations of motion

Considering the purpose of this study, we may use a seven-link model of a planar biped consisting of a trunk and two legs with three joints of hip, knee, and ankle in each leg, as shown in Fig. 1. It is assumed that all joints are revolute and actuated by rotational actuators co-located at the joints. It is also assumed that motion is confined in sagittal plane. We may describe the motion of biped using nine generalized coordinates; i.e., $\mathbf{q} = [q_1 \quad \dots \quad q_7 \quad x \quad z]^T$ as shown in Fig. 1.

Single support phase starts when toe of swing leg leaves the ground and ends when its heel comes in contact with the ground again. Considering that stance leg is virtually pivoted to the ground during this phase, one may write holonomic constraints, which state the condition for non-slipping contact, as follows:

$$\boldsymbol{\varphi}(\mathbf{q}) = \begin{bmatrix} z_A \\ z_B \\ x_B - c_1 \end{bmatrix} = \mathbf{0}, \tag{1}$$

where the subscripts A and B stand for heel and toe of stance leg, as shown in Fig. 2, and c_1 is a constant, which is the horizontal position of point B in the inertial coordinate system.

The forces applied on foot of stance leg can be replaced by two normal forces at heel (F_A^z) and toe (F_B^z) and a tangential force (F_{AB}^x). It means that contact forces during this phase can be shown as:

$$\mathbf{F} = \begin{bmatrix} F_A^z & F_B^z & F_{AB}^x \end{bmatrix}^T. \tag{2}$$

During one complete step, kinematic structure of biped changes due to the fact that DSP alternates with SSP. DSP starts when heel of swing leg comes in contact with ground and ends when the toe of stance leg leaves the ground. In this phase, the system has close-chain tree-like configuration. In this study, we assume that heel of stance leg leaves the ground as soon as DSP starts. In DSP, holonomic constraints

https://doi.org/10.1017/S0263574713000039 Published online by Cambridge University Press

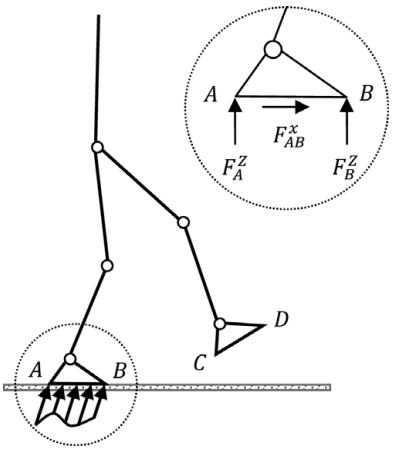

Fig. 2. Contact forces applied on the stance foot in SSP.

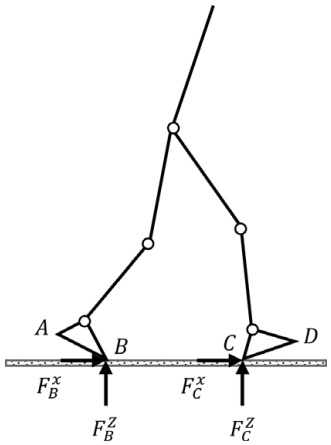

Fig. 3. Contact forces applied on the contact points in DSP.

are defined as follows:

$$\boldsymbol{\varphi}(\mathbf{q}) = \begin{bmatrix} x_B - c_2 \\ z_B \\ x_C - c_3 \\ z_C \end{bmatrix} = \mathbf{0}, \tag{3}$$

and contact forces are given as:

$$\mathbf{F} = \begin{bmatrix} F_B^x & F_B^z & F_C^x & F_C^z \end{bmatrix}^T, \tag{4}$$

where, in these relations, subscripts B and C stand for toe of rear leg and heel of front leg, as shown in Fig. 3, and c_2 and c_3 are some constants that are, respectively, the horizontal position of point B and C in the inertial coordinate system.

Equations of motion of this system can be obtained in general form as:

$$\mathbf{M}(\mathbf{q})\ddot{\mathbf{q}} + \mathbf{H}(\mathbf{q}, \dot{\mathbf{q}}) = \mathbf{B}\boldsymbol{\tau} + \mathbf{J}^{\mathbf{T}}\mathbf{F}, \tag{5}$$

where $\mathbf{M}(\mathbf{q})$ is a 9×9 symmetric inertia matrix; $\mathbf{H}(\mathbf{q}, \dot{\mathbf{q}})$ is a 9×1 array representing coriolis, gravitational, and centrifugal terms; $\mathbf{B}$ is a 9×6 matrix; and $\boldsymbol{\tau}$ is the 6×1 vector of input torques. Also, the matrix $\mathbf{J} = \partial\boldsymbol{\varphi}/\partial\mathbf{q}$ depicts Jacobian of holonomic constraints due to contact with the ground and $\mathbf{F}$ is the array of contact forces. One should note that $\mathbf{J}$ and $\mathbf{F}$ are different during SSP and DSP, which implies that we face two different sets of equations of motion during SSP and DSP.

Equation (5) can be rewritten in the following form:

$$\mathbf{M}(\mathbf{q})\ddot{\mathbf{q}} + \mathbf{H}(\mathbf{q}, \dot{\mathbf{q}}) = \mathbf{A}\,(\mathbf{q})\mathbf{u}, \tag{6}$$

where $\mathbf{A} = [\,\mathbf{B}\;\; \mathbf{J}^{\mathbf{T}}\,]$ and $\mathbf{u} = \begin{bmatrix} \boldsymbol{\tau} \\ \mathbf{F} \end{bmatrix}$.

2.2. *Stability condition*

As stated before it is sufficient that ZMP is located in the supporting polygon for a biped to have stable walking.[2] This means $x_A \le x_{ZMP} \le x_B$ during SSP and $x_B \le x_{ZMP} \le x_C$ during DSP. Writing moment equations around ZMP, one can show that this stability criterion is equivalent to having positive normal forces at contact points. In addition, to prevent slippage the normal forces applied on contact points must be large enough to supply enough friction force. Considering free body diagram shown in Fig. 2, the following conditions must hold to ensure stability and to prevent slippage during SSP:

$$\begin{cases} F_A^z \ge 0 \\ F_B^z \ge 0 \\ \mu\left(F_A^z + F_B^z\right) \ge \left|F_{AB}^x\right|. \end{cases} \tag{7}$$

One may rewrite the above inequality constraints in the following form:

$$\mathbf{DF} \ge \mathbf{0}, \tag{8}$$

where $\mathbf{F}$ is the vector of contact forces as defined in Eq. (2) and

$$\mathbf{D} = \begin{bmatrix} 1 & 0 & 0 \\ 0 & 1 & 0 \\ \mu & \mu & 1 \\ \mu & \mu & -1 \end{bmatrix}.$$

On the other hand, considering the free body diagram shown in Fig. 3, one can show that the following conditions must hold to ensure stability and non-slip condition in DSP:

$$\begin{cases} \mu F_B^z \ge \left|F_B^x\right| \\ \mu F_C^z \ge \left|F_C^x\right|. \end{cases} \tag{9}$$

As before, one might rewrite the above inequality constraints in the form of Eq. (8). In this case, however, $\mathbf{F}$ is the vector of contact forces defined in Eq. (4) and

$$\mathbf{D} = \begin{bmatrix} 1 & \mu & 0 & 0 \\ -1 & \mu & 0 & 0 \\ 0 & 0 & 1 & \mu \\ 0 & 0 & -1 & \mu \end{bmatrix}.$$

2.3. *Problem statement*

We may now state the minimum time problem as follows:

https://doi.org/10.1017/S0263574713000039 Published online by Cambridge University Press

Problem (1): Find the optimum path $\mathbf{q}^*(t)$ to minimize $\int_{t_i}^{t_f} dt$ subject to

$$\begin{gathered}\mathbf{M}(\mathbf{q})\ddot{\mathbf{q}} + \mathbf{H}(\mathbf{q}, \dot{\mathbf{q}}) = \mathbf{A}\,(\mathbf{q})\mathbf{u},\\ \mathbf{DF} \geq 0,\\ \boldsymbol{\varphi}(q) = \mathbf{0},\\ \boldsymbol{\tau}_{\min} \leq \boldsymbol{\tau} \leq \boldsymbol{\tau}_{\max},\end{gathered} \tag{10}$$

with initial and final conditions:

$$\mathbf{q}(t_i) = \mathbf{q}_i, \quad \mathbf{q}(t_f) = \mathbf{q}_f,$$

where $\boldsymbol{\tau}_{\min}$ and $\boldsymbol{\tau}_{\max}$ show saturation limits of the actuators. One should note that the matrices $\mathbf{A}$, $\mathbf{u}$, $\mathbf{D}$, $\mathbf{F}$, and $\boldsymbol{\varphi}$ are different during SSP and DSP as explained before.

This problem can be restated in a more convenient form by substituting Eq. (8) into Eq. (6). Let us define

$$\boldsymbol{\Lambda} = \mathbf{Tu}, \tag{11}$$

where

$$\boldsymbol{\Lambda} = \begin{bmatrix}\boldsymbol{\tau}\\ \mathbf{E}\end{bmatrix}, \ \mathbf{T} = \begin{bmatrix}\mathbf{I} & \mathbf{0}\\ \mathbf{0} & \mathbf{D}\end{bmatrix}$$

and $\mathbf{E}$ depicts a 4×1 vector that equals to $\mathbf{DF}$ as defined in Eq. (8).

Considering that $\mathbf{A}$ is a 9×9 non-singular matrix in SSP, one may pre-multiply Eq. (6) by $\mathbf{TA}^{-1}$ and substitute $\mathbf{E} = \mathbf{DF}$ to obtain

$$\bar{\mathbf{M}}(\mathbf{q})_{10\times 9}\ddot{\mathbf{q}} + \bar{\mathbf{H}}(\mathbf{q}, \dot{\mathbf{q}})_{10\times 1} = \boldsymbol{\Lambda}_{10\times 1}, \tag{12}$$

where $\bar{\mathbf{M}} = \mathbf{TA}^{-1}\mathbf{M}$ and $\bar{\mathbf{H}} = \mathbf{TA}^{-1}\mathbf{H}$.

Equation (12) shows 10 equations that can be solved along with three holonomic constraints, Eq. (1), to find $\mathbf{q}_{9\times 1}$ and $\mathbf{E}_{4\times 1}$ as unknown.

In a similar way, for DSP we may substitute $\mathbf{u} = \mathbf{T}^{-1}\boldsymbol{\Lambda}$ from Eq. (11) into Eq. (6) to get

$$\mathbf{M}(\mathbf{q})_{9\times 9}\ddot{\mathbf{q}} + \mathbf{H}(\mathbf{q}, \dot{\mathbf{q}})_{9\times 1} = \bar{\mathbf{A}}(\mathbf{q})_{9\times 10}\boldsymbol{\Lambda}_{10\times 1}, \tag{13}$$

where $\bar{\mathbf{A}} = \mathbf{AT}^{-1}$.

One should note that in DSP, $\mathbf{T}$ is a 10×10 non-singular matrix. Equation (13) shows nine equations that can be solved along with four holonomic constraints, Eq. (3), to give $\mathbf{q}_{9\times 1}$ and $\mathbf{E}_{4\times 1}$ as unknown.

Considering these extended equations of motion, Eqs. (12) and (13), one may restate the minimum time problem in the following form:

Problem (2): Find the optimum path $\mathbf{q}^*(t)$ to minimize $\int_{t_i}^{t_f} dt$ subject to

$$\begin{gathered}\begin{cases}\bar{\mathbf{M}}(\mathbf{q})\ddot{\mathbf{q}} + \bar{\mathbf{H}}(\mathbf{q}, \dot{\mathbf{q}}) = \boldsymbol{\Lambda} & \text{for SSP}\\ \mathbf{M}(\mathbf{q})\ddot{\mathbf{q}} + \mathbf{H}(\mathbf{q}, \dot{\mathbf{q}}) = \bar{\mathbf{A}}(\mathbf{q})\boldsymbol{\Lambda} & \text{for DSP}\end{cases},\\ \boldsymbol{\varphi}(\mathbf{q}) = \mathbf{0},\\ \boldsymbol{\Lambda}_{\min} \leq \boldsymbol{\Lambda} \leq \boldsymbol{\Lambda}_{\max},\end{gathered} \tag{14}$$

with initial and final conditions:

$$\mathbf{q}(t_i) = \mathbf{q}_i, \ \mathbf{q}(t_f) = \mathbf{q}_f.$$

Considering the actuator limits $\boldsymbol{\tau}_{\min} \leq \boldsymbol{\tau} \leq \boldsymbol{\tau}_{\max}$ and limits due to stability criterion defined in Eq. (8) as $\mathbf{E} \geq 0$, the limits on $\boldsymbol{\Lambda}$ can be written as:

$$\boldsymbol{\Lambda}_{\min} = \begin{bmatrix}\boldsymbol{\tau}_{\min}\\ \mathbf{0}\end{bmatrix}, \ \boldsymbol{\Lambda}_{\max} = \begin{bmatrix}\boldsymbol{\tau}_{\max}\\ \infty\end{bmatrix}.$$

As explained in the previous section, solution of this problem may result in unacceptable solutions from practical point of view for walking purpose. To circumvent this problem, we should add some kinematic constraints necessary for an acceptable walking pattern. In the next section, we develop such kinematic constraints.

3. Kinematic Constraints of Natural Walking

Considering that moving hip joint in horizontal direction might be regarded as main objective of walking, one might try to express motion of the whole body as functions of that in such a way to comply with physical constraints of walking. To this end, we might define the non-dimensional parameter of motion, s, as:

$$s = \frac{x - x_i}{D_s}, \tag{15}$$

where x and x_i are, respectively, the horizontal position of hip joint and its value at the beginning of SSP and D_s is the step length of walking as shown in Fig. 4. Equation (15) shows that the value of s varies between zero and one during one step. The value of s at the end of SSP is $s_c = (x_c - x_i)/D_s$, in which x_c is the horizontal position of hip joint at the end of SSP. The value of s_c also depicts the ratio of SSP of the whole step.

Now, recalling that the system in SSP and DSP has respectively six and five degrees of freedom, to have a fixed pattern of motion we need some kinematic constraints in the form of:

$$g_i(\mathbf{q}, s) = 0, \quad \begin{cases} i = 1, \ldots, 5 & \text{for SSP}\\ i = 1, \ldots, 4 & \text{for DSP}\end{cases}. \tag{16}$$

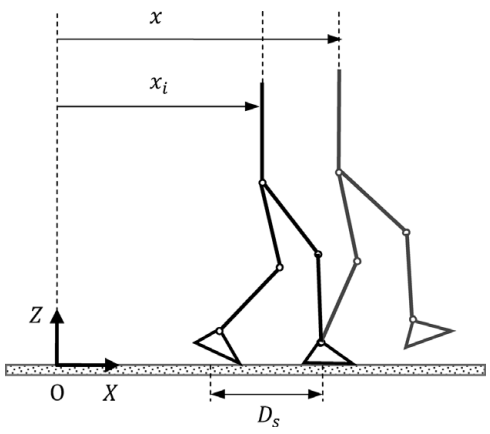

Fig. 4. Position of hip joint in the inertial coordinate system.

https://doi.org/10.1017/S0263574713000039 Published online by Cambridge University Press

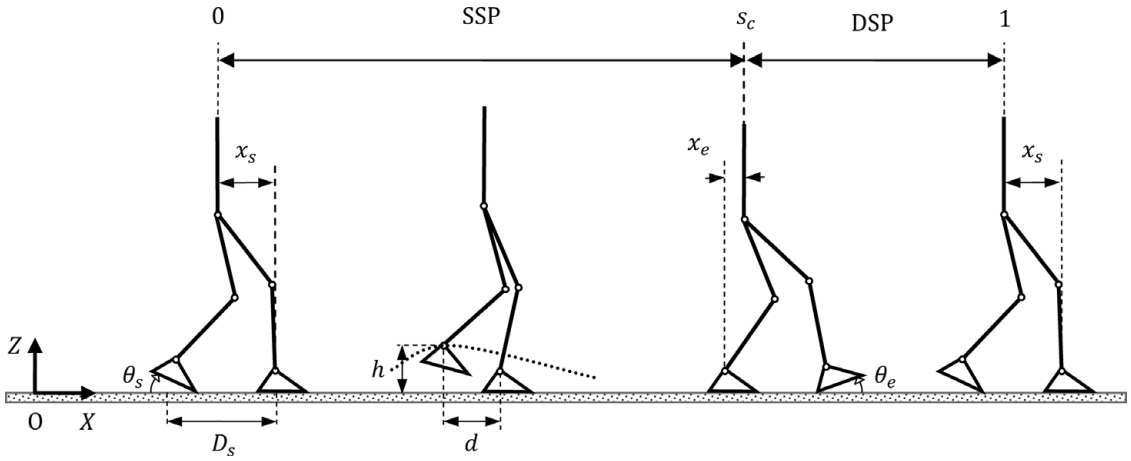

Fig. 5. Motion pattern of biped robot during one step.

These kinematic constraints can be defined by assuming natural motion for trunk, hip, and ankle joints. In another word, we try to define geometric trajectories for trunk, vertical motion of hip joint, horizontal and vertical motion of ankle joint of swing leg, and angle of both foots during a step in terms of non-dimensional horizontal position of hip joint, s, defined in Eq. (15). We consider some polynomials in terms of the parameter s and then the coefficients of these polynomials are obtained by choosing proper values of geometric constants and enforcing some constraints in accordance with natural walking.

We consider vertical motion of hip joint such that it is at the highest level in the middle of SSP and at the lowest in the middle of DSP. Such conditions are expressed as follows:

$$z(s) = \begin{cases} H_{\max} & s = 0.5s_c \\ H_{\min} & s = s_c + 0.5(1 - s_c) \end{cases}. \tag{17}$$

To satisfy these two conditions, we may use two polynomials of second order for z as follows:

$$z(s) = \begin{cases} \alpha(s - 0.5s_c)^2 + H_{\max} & s \le s_c \\ \beta(s - s_c - 0.5(1 - s_c))^2 + H_{\min} & s > s_c \end{cases}. \tag{18}$$

Coefficients α and β, in the above relation, are obtained such that the continuity conditions in position and velocity are satisfied.

It is also assumed that trunk remains vertical during motion, which means:

$$q_4(s) = 0. \tag{19}$$

To design a suitable trajectory for angle of foots, we use a fifth-order polynomial in DSP for q_1 satisfying the following geometric conditions:

$$q_1(s) = \begin{cases} 0 & s = s_c \\ \theta_s & s = 1 \end{cases}, \quad \dot{q}_1(s) = \begin{cases} 0 & s = s_c \\ 0 & s = 1 \end{cases},$$
$$\ddot{q}_1(s) = \begin{cases} 0 & s = s_c \\ 0 & s = 1 \end{cases}, \tag{20}$$

and two fifth-order polynomials in terms of s for q_7 during SSP and DSP to satisfy the following requirements:

$$q_7(s) = \begin{cases} \theta_s & s = 0 \\ \theta_e & s = s_c \\ 0 & s = 1 \end{cases}, \quad \dot{q}_7(s) = \begin{cases} 0 & s = 0 \\ 0 & s = s_c \\ 0 & s = 1 \end{cases},$$
$$\ddot{q}_7(s) = \begin{cases} 0 & s = 0 \\ 0 & s = s_c \\ 0 & s = 1 \end{cases}, \tag{21}$$

where θ_s and θ_e are, respectively, foot angle of swing leg at the beginning and end of SSP, as shown in Fig. 5.

The two last kinematic constraints that must be determined are horizontal and vertical position of ankle joint of swing leg. To define them, we use a fifth-order polynomial in terms of s for its horizontal position, which should satisfy the following requirements:

$$x_a(s) = \begin{cases} x_i - x_s - D_s + l_f - l_f\cos(\theta_s) + l_a\sin(\theta_s) & s = 0 \\ x_c - x_e + D_s - l_h + l_h\cos(\theta_e) + l_a\sin(\theta_e) & s = s_c \end{cases},$$
$$\dot{x}_a(s) = \begin{cases} 0 & s = 0 \\ 0 & s = s_c \end{cases}, \quad \ddot{x}_a(s) = \begin{cases} 0 & s = 0 \\ 0 & s = s_c \end{cases}, \tag{22}$$

where x_s and x_e are, respectively, horizontal position of hip joint at the beginning and end of SSP measured from stance ankle joint, as shown in Fig. 5. Also, l_h and l_f show the length of heel and toe portions of foot and l_a is the height of the foot (see Fig. 6).

On the other hand, vertical motion at ankle joint is not normally symmetric during the motion. The vertical motion of ankle joint can be defined by two cubic polynomials in terms of horizontal position of ankle joint, x_a. The coefficients of these polynomials should be computed in such a way that the following physical constraints are satisfied and the first and second derivatives of the resulting polynomials be continuous.

$$z_a(x_a(s)) = \begin{cases} l_f\sin(\theta_s) + l_a\cos(\theta_s) & s = 0 \\ h & x_a = d, \\ -l_h\sin(\theta_e) + l_a\cos(\theta_e) & s = s_c \end{cases}$$
$$\dot{z}_a(x_a(s)) = 0 \quad x_a = d, \tag{23}$$

https://doi.org/10.1017/S0263574713000039 Published online by Cambridge University Press

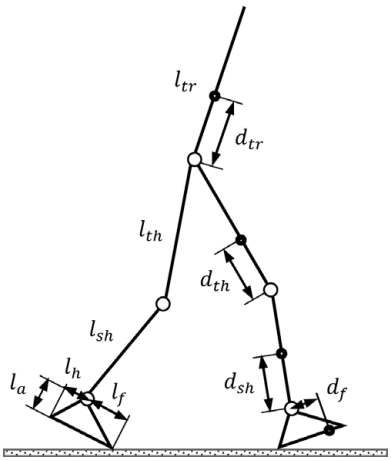

Fig. 6. Schematic diagram of biped dimension.

Table I. The walking parameters of the biped robot.

Parameters	Values
x_s	$-0.545 s_c D_s$
x_e	$0.455 s_c D_s$
θ_s	$0.28 D_s/(l_a + l_{sh} + l_{th})$
θ_e	$-0.28 D_s/(l_a + l_{sh} + l_{th})$
d	$-0.37 D_s$
h	0.2
$H_{\max}$	$\sqrt{(l_{sh} + l_{th})^2 - (0.5 D_s)^2} + l_a - 0.06$
$H_{\min}$	$H_{\max} - 0.02$

where (d, h) shows the position of the highest point of the swing foot as shown in Fig. 5.

Walking parameters in above relations are some arbitrary values that are normally chosen to comply with normal walking pattern. A typical choice of these parameters is given in Table I. The coefficients of relations given in this table are chosen to yield a normal walking pattern. Moreover, the value of $H_{\max}$ and $H_{\min}$ are choosing to get as close as possible to the situation of straight knee walking, while avoiding singularity.

Equations (17)–(23) impose geometric constraints that incorporate physical conditions of natural walking pattern. So these relations must also be satisfied by the minimum time solution. Considering these relations, the final form of minimum time problem is stated in the next section and the solution algorithm is also presented. One should note that these kinematic constraints have fixed the pattern of motion. Indeed, it is not the coefficients of the polynomials but the parameter $s^*(t)$ that is determined by the minimum time solution. If $s^*(t)$ is known, the whole path is known.

4. Minimum Time Solution

To solve the minimum time problem stated in the previous section, we first try to restate it in terms of non-dimensional path parameter s. Defining $\mathbf{X} = [\, q_4 \quad q_7 \quad x \quad z \quad x_a \quad z_a \,]^T$ for SSP and $\mathbf{X} = [\, q_1 \quad q_4 \quad q_7 \quad x \quad z \,]^T$ for DSP as the work space trajectories that are to be followed, one can write them in terms of s as follows:

$$\mathbf{X} = \mathbf{f}(s). \tag{24}$$

On the other hand, direct kinematic equations of biped describe $\mathbf{X}$ in terms of $\mathbf{q}$ as follows:

$$\mathbf{X} = \mathbf{p}(\mathbf{q}). \tag{25}$$

Substituting $\mathbf{X}$ from Eq. (24) into Eq. (25) and solving for $\mathbf{q}$ yields:

$$\mathbf{q} = \mathbf{p}^{-1}(\mathbf{f}(s)) = \mathbf{q}(s). \tag{26}$$

Differentiating Eq. (26) with respect to time, one gets $\dot{\mathbf{q}}$ and $\ddot{\mathbf{q}}$ as follows:

$$\dot{\mathbf{q}} = \mathbf{q}'(s)\dot{s}, \tag{27}$$

$$\ddot{\mathbf{q}} = \mathbf{q}''(s)\dot{s}^2 + \mathbf{q}'(s)\ddot{s}, \tag{28}$$

where $(.)'$ and $(.)''$ denote first and second derivatives with respect to s.

Plugging these equations in extended form of equations of motion, Eqs. (12) and (13), these equations can be written as:

$$\bar{\mathbf{c}}(s)\ddot{s} + \bar{\mathbf{d}}(s)\dot{s}^2 + \bar{\mathbf{e}}(s) = \mathbf{\Lambda}, \tag{29}$$

$$\mathbf{c}(s)\ddot{s} + \mathbf{d}(s)\dot{s}^2 + \mathbf{e}(s) = \bar{\mathbf{A}}(s)\mathbf{\Lambda}. \tag{30}$$

Now we may restate the minimum time problem as:

Problem (3): Find the optimum path $s^*(t)$ to minimize $\int_{t_i}^{t_f} dt$ subject to

$$\begin{cases} \bar{\mathbf{c}}(s)\ddot{s} + \bar{\mathbf{d}}(s)\dot{s}^2 + \bar{\mathbf{e}}(s) = \mathbf{\Lambda} & 0 \le s \le s_c \\ \mathbf{c}(s)\ddot{s} + \mathbf{d}(s)\dot{s}^2 + \mathbf{e}(s) = \bar{\mathbf{A}}(s)\mathbf{\Lambda} & s_c < s \le 1 \end{cases},$$

$$\mathbf{\Lambda}_{\min} \le \mathbf{\Lambda} \le \mathbf{\Lambda}_{\max}, \tag{31}$$

with initial and final conditions:

$$s(t_i) = 0, \; s(t_f) = 1.$$

Problem (3) is presented in a form similar to what was first addressed by Bobrow *et al.*[22] for serial manipulators moving on a specified path and later on solved by Moon and Ahmad[27,28] and Bobrow *et al.*[29] for parallel manipulators. According to them, solution to this problem is bang-bang in terms of $\ddot{s}$, which leaves the following two main steps to complete the solution.

(1) To find the maximum and minimum value of $\ddot{s}$ at each point along the path.
(2) To find the switching points.

Thanks to the fact that a higher solution in phase plane takes shorter time to be accomplished, they suggested a phase-plane analysis to solve the problem. They also showed that due to inequality constraints, there would be a specific value of $\dot{s}$ for each point of the path beyond which no combination of actuator torques could keep the manipulator

https://doi.org/10.1017/S0263574713000039 Published online by Cambridge University Press

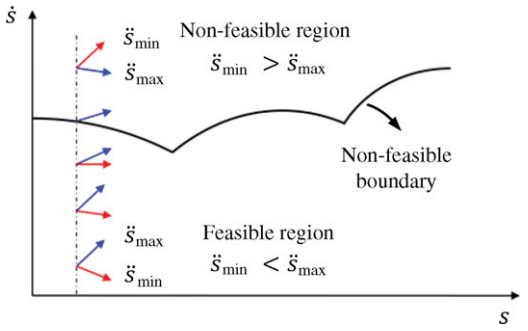

Fig. 7. (Colour online) Categorization of phase plane according to acceleration bounds.

on the specified path. These points form the boundary of non-feasible region in phase plane, as entitled by Bobrow *et al.*[22] In another words, as Fig. 7 shows, one might categorize points of phase plane as follows:

(1) Feasible points $(s, \dot{s})$ from which the system can move with a variety of accelerations $\ddot{s}_{\min} \leq \ddot{s} \leq \ddot{s}_{\max}$.
(2) Non-feasible points for which $\ddot{s}_{\max} < \ddot{s}_{\min}$, which means there is no solution satisfying the inequality constraints.
(3) Points on NFB for which $\ddot{s}_{\min} = \ddot{s}_{\max}$ is the only possible acceleration along the path.

Establishment of NFB is a very crucial step in finding switching curve and the minimum time solution.

To find maximum or minimum acceleration at a desired point $(s_d, \dot{s}_d)$, one should solve the following linear programming problem:

L (1): Find the control input $\boldsymbol{\tau}$ to maximize or minimize $\ddot{s}$ subject to:

$$\begin{cases} \bar{\mathbf{c}}(s_d)\ddot{s} + \bar{\mathbf{d}}(s_d)\dot{s}_d^2 + \bar{\mathbf{e}}(s_d) = \boldsymbol{\Lambda} & 0 \leq s_d \leq s_c \\ \mathbf{c}(s_d)\ddot{s} + \mathbf{d}(s_d)\dot{s}_d^2 + \mathbf{e}(s_d) = \bar{\mathbf{A}}(s_d)\boldsymbol{\Lambda} & s_c < s_d \leq 1 \end{cases},$$
$$\boldsymbol{\Lambda}_{\min} \leq \boldsymbol{\Lambda} \leq \boldsymbol{\Lambda}_{\max}. \qquad (32)$$

To establish the boundary of non-feasible region, it is necessary to find the value of $\dot{s}$ that makes $\ddot{s}_{\min} = \ddot{s}_{\max}$ for all values of s. Such a procedure for constructing NFB is very time consuming and tedious. Pfeiffer and Johanni[23] introduced a method that directly gives $\ddot{s}_{\max}$, $\ddot{s}_{\min}$, and $\dot{s}^2_{\max}$ at each value of s for serial manipulators. They also proved that the curve defined by $(s, \dot{s}_{\max})$ is the boundary of non-feasible region. This way they gave a direct method to establish NFB for serial manipulators. On the other hand, a similar problem was studied by Sadigh *et al.*[32] for parallel manipulators. Details of these approaches and how they can be applied to our system are given in the Appendix.

To establish the switching curve and present a solution algorithm, we need to know the nature of points on NFB. Points on NFB are categorized as sink or source depending on whether the slope of solution curve in phase plane, $\ddot{s}/\dot{s}$, is greater or smaller than slope of NFB (see Fig. 8(a)). Any solution starting from a source continues in the feasible region, whereas any solution starting from a sink immediately leaves the feasible region. On the other hand, there is one feasible solution trajectory that ends up to a sink; however, no feasible solution trajectory ends up to a source. It means that both forward and backward integrations from a sink to source point on NFB would result in feasible solution trajectories. These points being called critical points are candidates of being switching points on NFB (more details could be found in refs. [23, 25].)

Another point that is worthy of attention is that the value of $\dot{s}$ at the beginning and end of the step is not known. However, to comply with periodicity condition $\dot{s}_i = \dot{s}_f$ and to have the fastest motion, they should take the maximum possible values. The method of choosing $\dot{s}_i$ and $\dot{s}_f$ is described in more detail in the solution algorithm of the problem.

4.1. Phase-plane algorithm

To find the minimum time path and appropriate initial and final conditions for $\dot{s}$, the following steps should be taken:

Step 1: Construct NFB in phase plane either using a search algorithm based on L (1) or by the method described in the Appendix (see also Fig. 8).

Step 2: Find critical points on NFB where the points on NFB changes from sink to source, e.g., points C_1, C_2, and C_3 in Figs. 8(a) and 8(b). These points are candidates of being switching points on NFB.

Step 3: From lowest critical point, C_2, integrate backward in time with minimum acceleration until either the line of $s = 0$ is crossed or $\ddot{s}_{\min}$ becomes greater than $\ddot{s}_{\max}$, i.e., solution trajectory enters non-feasible region—point b_1 in Figs. 8(a) and 8(b). Considering the fact that solution trajectories in phase plane do not cross each other, any solution that starts above this line can not continue in the feasible region and eventually ends up in the non-feasible region. The area between this trajectory (B_1) and NFB is called the trapped area (A^T). It means that any critical point located in this area is of no importance and should be ignored.

Step 4: From point C_2 integrate forward in time with maximum acceleration until either the line of $s = 1$ is crossed, point b_2 in Fig. 8(a), or the solution trajectory, B_2, crosses NFB at point b_2 (Fig. 8(b)). In this case the area above line B_2 is a locked area (A^L), which means no solution trajectory that starts in feasible region can enter this area. This means that any critical point that is located in this area can never be reached and must be ignored, e.g., point C_3 in Figs. 8(a) and 8(b). Point C_2 would be one of the switching points on NFB.

Step 5: Repeat Steps 3 and 4 from the lowest neighboring critical point outside trapped and locked area, like point C_1 in Figs. 8(a) and 8(b), to generate solution trajectories B_3 and B_4. The point S_2 in Fig. 8(a) or S_3 in Fig. 8(b) in which B_4 crosses B_1 is another switching point. Continue this procedure until either both lines of $s = 0$ and $s = 1$ is crossed, like Fig. 8(a), or there remains no critical point outside trapped and locked area, like the case shown in Fig. 8(b). After doing this, lowest portion of solution curves B_1 to B_n generates the switching curve, e.g., curve $b_3\, C_1\, S_2\, C_2\, b_2$ in Fig. 8(a) and curve $b_3\, C_1\, S_3\, C_2\, b_2$ in Fig. 8(b).

Switching curve, which is itself a solution curve, divides the phase plane into admissible and non-admissible areas, i.e., any motion starting from a point below this curve remains in the feasible region; however, any motion starting from a point above this curve will eventually end up in the

https://doi.org/10.1017/S0263574713000039 Published online by Cambridge University Press

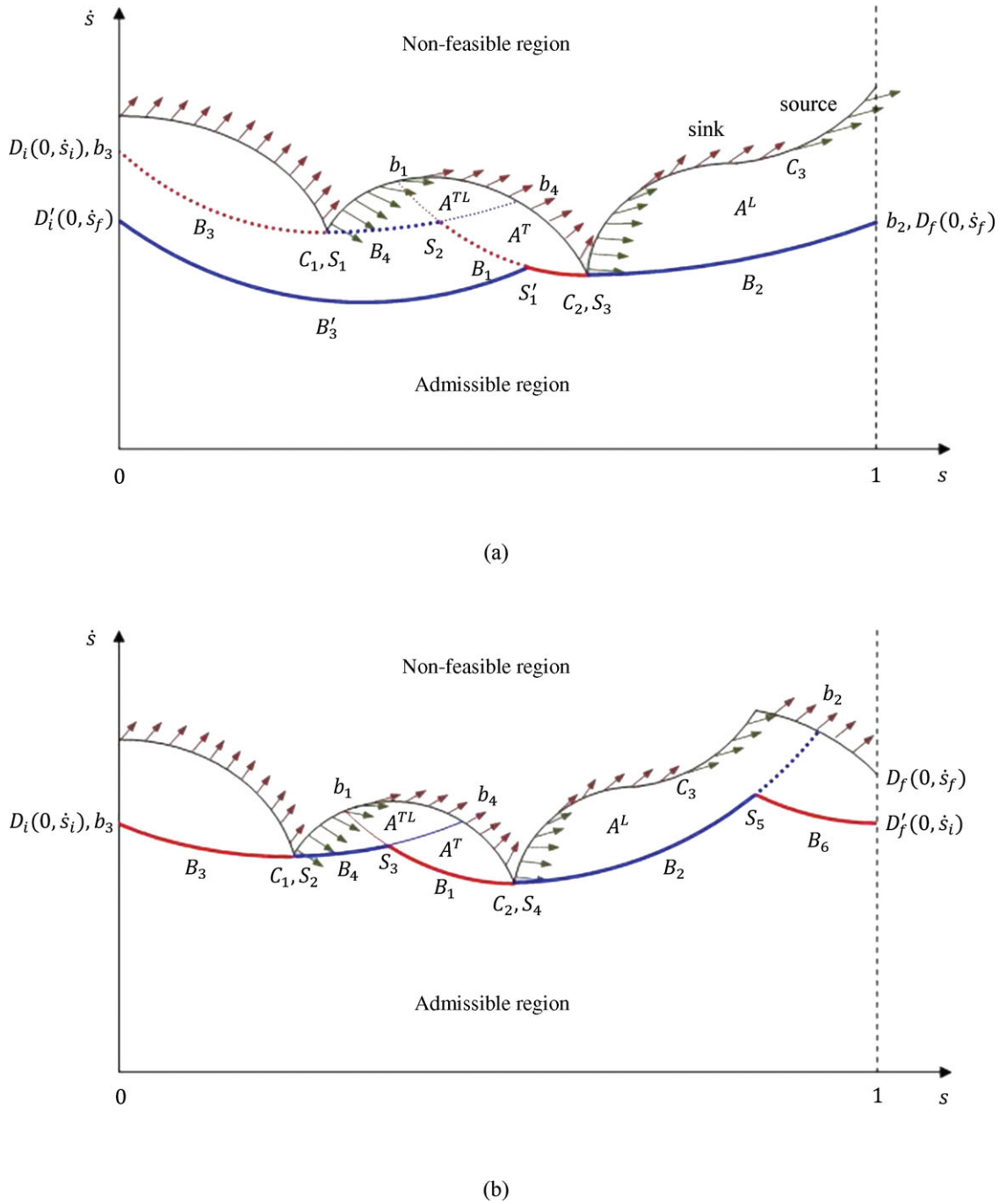

Fig. 8. (Colour online) Schematic diagram of the solution curve.

non-feasible region. It means that this curve would be the highest feasible solution curve in the phase plane. It gives the idea that the minimum time solution can be found by integrating forward (backward) in time with $\ddot{s}_{\max}$ ($\ddot{s}_{\min}$) from initial (final) condition until this switching curve is crossed.

It is clear from Figs. 8(a) and 8(b) that the maximum achievable values of $\dot{s}$ at $s = 0$ and $s = 1$ are $\dot{s}_i$ and $\dot{s}_f$ for the case that switching curve intersects lines $s = 0$ or $s = 1$, respectively, e.g., points D_i and D_f in Fig. 8(a) and point D_i in Fig. 8(b). The maximum achievable $\dot{s}$, on the other hand, equals $\dot{s}$ at intersection of NFB with lines $s = 0$ and $s = 1$ in cases where switching curve does not cross lines $s = 0$ or $s = 1$, e.g., point D_f in Fig. 8(b). Although these initial and final points are feasible, they do not generally satisfy periodicity constraint of $\dot{s}_i = \dot{s}_f$. This problem is resolved by taking the next step.

Step 6: Choose the minimum of $\dot{s}_i$ and $\dot{s}_f$ as the initial and final values for $\dot{s}$ (see points D_i' and D_f in Fig. 8(a) and D_i and D_f' in Fig. 8(b)). Integrate from initial or final condition that is changed until the solution curve crosses the switching curve, i.e., points S_1' in Fig. 8(a) and S_5 in Fig. 8(b).

The solution that starts from initial point and follows on the switching curve and ends up at the final point is the minimum time path, i.e., curve $D_i'\, S_1'\, C_2\, D_f$ in Fig. 8(a) and curve $D_i\, C_1\, S_3\, C_2\, S_5\, D_f'$ in Fig. 8(b). It should be noted that for the first and last step of walking, the periodicity constraint is removed and $\dot{s}_i = 0$ or $\dot{s}_f = 0$ will be used accordingly.

https://doi.org/10.1017/S0263574713000039 Published online by Cambridge University Press

Table II. The physical parameters of the biped robot.

Links	Feet	Shin	Thigh	Trunk
Length (m)	0.23	0.3	0.3	0.5
Mass (kg)	3.3	5.7	10	30
Inertia (kg.m^2)	0.01	0.02	0.03	1.7
Mass center position (m)	0	0.15	0.15	0.25
Feet characteristics		l_h	l_f	l_a
		0.1 m	0.13 m	0.1 m
Motors		Ankle	Knee	Hip
Torque max (N.m)		70	100	70

5. Numerical Examples

In this section, two numerical examples are presented. The objective of the first example is twofold: first, to show how the method works and second to show the effectiveness of the method by comparing the maximum achievable speed with what was obtained in a previous study by Sadigh and Mansouri[21] for the same biped. The next example is adopted from a recent work[20] on optimal path of biped motion to show the ability of the proposed algorithm by comparison of obtained results.

5.1. Example 1

To illustrate how the method works, in this section the proposed algorithm is applied to solve the minimum time motion of a seven-link biped. Physical parameters of biped and actuator limits are given in Table II. The position of mass center of links and their length are shown in Fig. 6.

It is assumed that $s_c = 0.80$, $D_s = 0.45$m, and $\mu = 0.2$. Considering the inertial coordinate system shown in Fig. 5 is located beneath the ankle joint of the stance foot, the value of x_i equals x_s. By this assumption, Eq. (15) yields:

$$x(s) = 0.45s - 0.196. \tag{33}$$

One should note that s is a non-dimensional parameter, which means that it has no unit of measurement. Substituting physical and walking parameters from Tables I and II, respectively, into the geometric conditions given by Eqs. (17)–(23) and solving linear equation, the polynomial coefficients of geometric trajectories defined in Section 3 can be calculated, which gives:

$$z(s) = \begin{cases} -0.1(s-0.4)^2 + 0.596 & s \le 0.8 \\ 0.4(s-0.9)^2 + 0.576 & s > 0.8 \end{cases}, \tag{34}$$

$$q_1(s) = 3375(s-0.8)^5 - 1687(s-0.8)^4 + 225(s-0.8)^3 \quad s > 0.8, \tag{35}$$

$$q_7(s) = \begin{cases} -6.592s^5 + 13.184s^4 - 7.031s^3 + 0.18 & s \le 0.8 \\ 3375(s-0.8)^5 - 1687(s-0.8)^4 + 225(s-0.8)^3 - 0.18 & s > 0.8 \end{cases}, \tag{36}$$

$$x_a(s) = 15.756s^5 - 31.512s^4 + 16.806s^3 - 0.430 \quad s \le 0.8, \tag{37}$$

$$z_a(x_a(s)) = \begin{cases} 2.982x_a^3 + 1.145x_a^2 + 0.133x_a + 0.204 & x_a \le -0.167 \\ 0.194x_a^3 - 0.253x_a^2 - 0.101x_a + 0.190 & x_a > -0.167 \end{cases} \quad s \le 0.8. \tag{38}$$

The boundary of non-feasible region, which is calculated using the Pfeiffer polygons, is shown in Fig. 9. Values of $\ddot{s}/\dot{s}$ and slope of NFB are compared in Fig. 10 that shows that the behavior of the boundary changes from sink to source at six critical points: $s = 0.075, 0.559, 0.665, 0.829, 0.841$, and 0.968. These points, as explained before, are candidates of being switching points. The switching curve is established by backward integration with $\ddot{s}_{\min}$ and forward integration with $\ddot{s}_{\max}$ from point $C_1(0.075, 1.599)$, the lowest critical point in the phase plane, which results in branches B_1 and B_2, as shown in Fig. 9. Solution curve B_1 crosses line $s = 0$ at $\dot{s}_i = 1.989\text{s}^{-1}$, which gives the maximum possible speed of hip joint at the beginning of SSP. As parameter $\dot{s}$ shows time derivative of a non-dimensional parameter, its unit would be

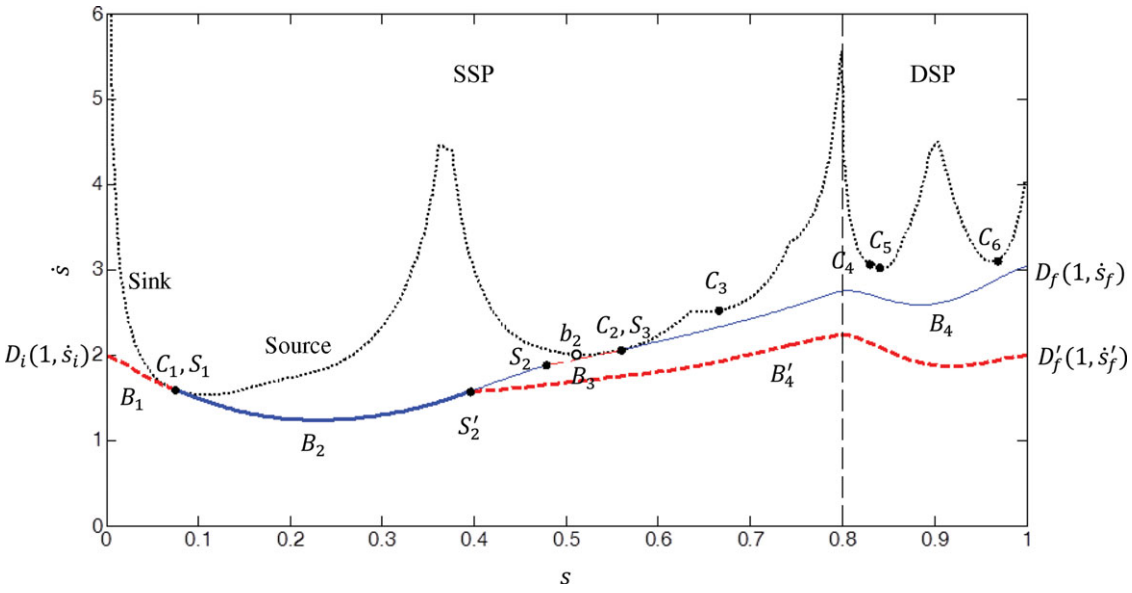

Fig. 9. (Colour online) Schematic diagram of the NFB and solution curve.

https://doi.org/10.1017/S0263574713000039 Published online by Cambridge University Press

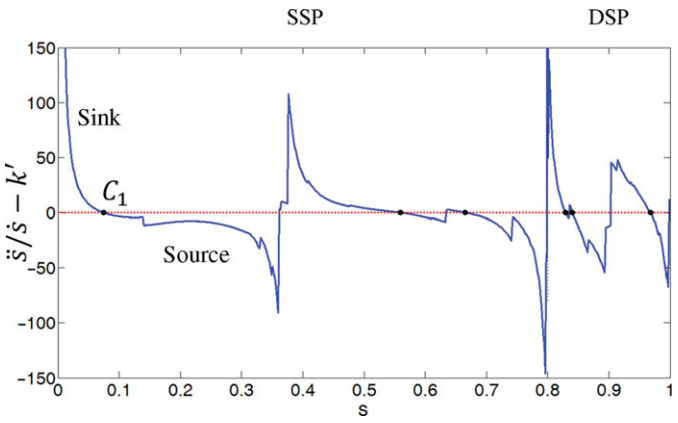

Fig. 10. (Colour online) The difference between $\ddot{s}/\dot{s}$ and slope of NFB.

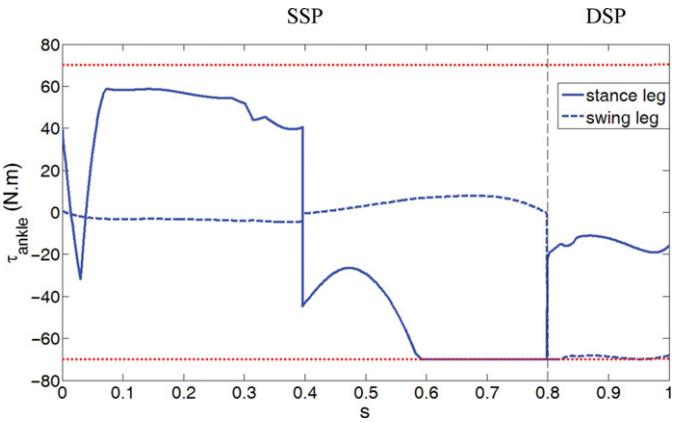

Fig. 11. (Colour online) Ankle torques.

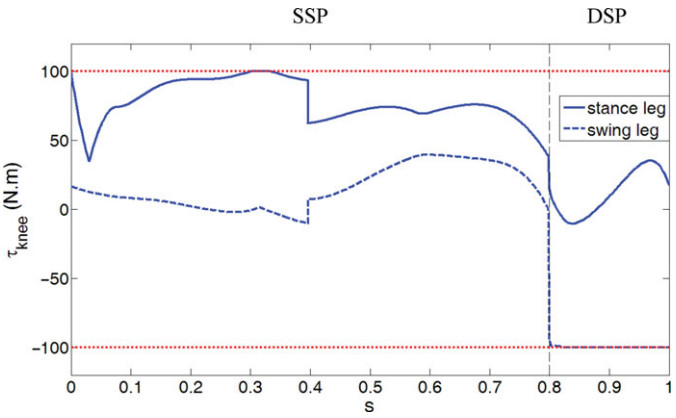

Fig. 12. (Colour online) Knee torques.

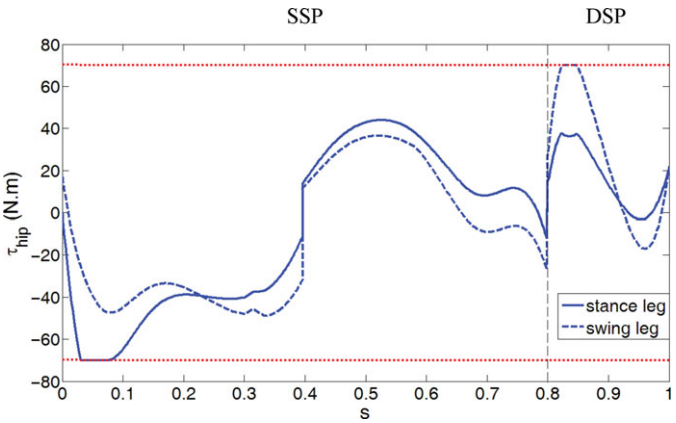

Fig. 13. (Colour online) Hip torques.

s^{-1}. Branch B_2, on the other hand, enters non-feasible region at point $b_2(0.519, 2.009)$. The algorithm continues from the next lowest critical point, $C_2(0.559, 2.060)$. Solution curve B_3 that is obtained by backward integration with $\ddot{s}_{\min}$ crosses branch B_2 at point $S_2(0.478, 1.882)$, which is a switching point. The forward path from point C_2, on the other hand, does not cross NFB, but crosses line $s = 1$ at $\dot{s}_f = 3.039$, which gives the maximum possible speed of hip joint at the end of step. An interesting fact is that in this problem four critical points—C_3, C_4, C_5, and C_6—are not switching points. This is due to the fact that the area between line B_4 and NFB is the locked area, which means no solution starting below line B_4 can enter this area.

As the last step, we locate $D'_f(1, \dot{s}'_f)$ such that $\dot{s}'_f = \min(\dot{s}_i, \dot{s}_f)$ and integrate backward in time until the switching curve is intersected at $S'_2(0.396, 1.575)$. The solution curve shown in Fig. 9 is depicted by curve $D_i C_1 S'_2 D'_f$, which is the highest admissible path in the phase plane that satisfies periodicity constraint.

In summary, the minimum time motion during a step starts at hip joint speed of $\dot{s}_i = 1.989$ and decelerate to $\dot{s}_1 = 1.599$ in which the acceleration is switched to its maximum value to reach a speed of $\dot{s}'_2 = 1.575$. The motion again switches to the minimum acceleration at this point and ends up at $\dot{s}'_f = 1.989$. One should note that moving with minimum acceleration does not, in general, mean decelerating and *vice versa*. In fact, depending on the situation, $\ddot{s}_{\min}$ might take positive values while it should normally be negative, and on the other hand, $\ddot{s}_{\max}$ may, in some cases, become negative.

This problem needs two switches, which are $S_1(0.075, 1.599)$ and $S'_2(0.396, 1.575)$, as shown in Fig. 9. The maximum admissible speed at the beginning and end of a step is also calculated as $\dot{s} = 1.989$. The time elapse for this step is calculated as 0.603 s, which is almost 40% less than the minimum time reported by Sadigh and Mansouri,[21] calculated for the same biped based on a parameter study. Considering that $D_s = 0.45$m means the maximum achievable speed of this biped would be $V_{\max} = 2.69$km/h.

Figures 11–13 show actuator torques of stance and swing leg during one step, where the solid line corresponds to the stance leg and dotted line corresponds to the swing leg. Figures 14 and 15 show how stability constraints given by Eqs. (7) and (9) are satisfied during the motion. Figure 16 shows ZMP track during the motion that is, as expected, located within the stable region.

As it is visible from Figs. 11–15, at each instance at least one of the constraints—either actuator bounds or stability and non-slip constraints—is saturated in SSP while two of them are saturated in DSP. In another words, moving with maximum or minimum acceleration is limited at least by one of the constraints for SSP and two of them for DSP. Figure 17 shows different intervals in which each constraint is saturated. As shown, non-slipping and ankle actuator bounds

https://doi.org/10.1017/S0263574713000039 Published online by Cambridge University Press

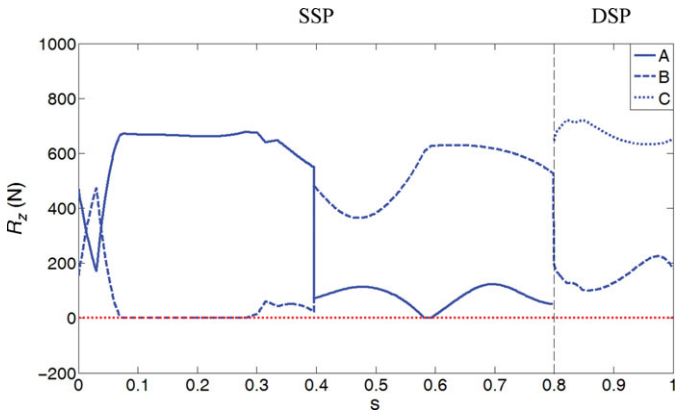

Fig. 14. (Colour online) Normal ground reaction forces.

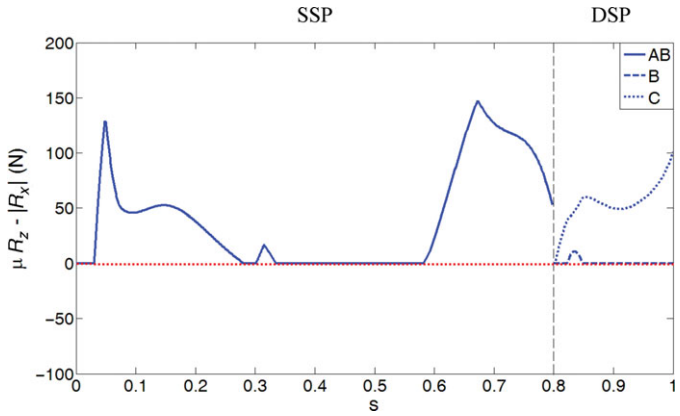

Fig. 15. (Colour online) Non-slip constraints.

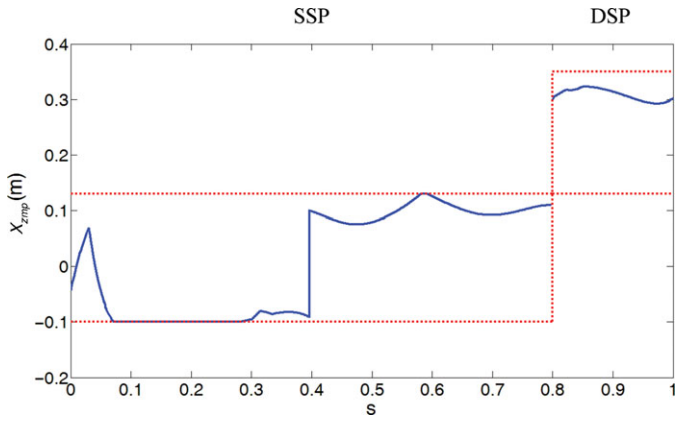

Fig. 16. (Colour online) ZMP diagram and stable region.

are the two most important constraints for this biped. A stick diagram of this motion is shown in Fig. 18.

This solution can be used either as an upper limit for achievable speed by this biped or as a guide to design a near-minimum time motion trajectory that could be implemented practically. Design and implementation of such practical near-minimum time solution could be considered as future works to be done. Another point that is worth mentioning is that this minimum time solution is an off-line procedure, which means computation cost is another interesting subject. That computation cost is not a critical issue in that. However, as a reference value we should mention that it takes 16.91 s to perform all forward and

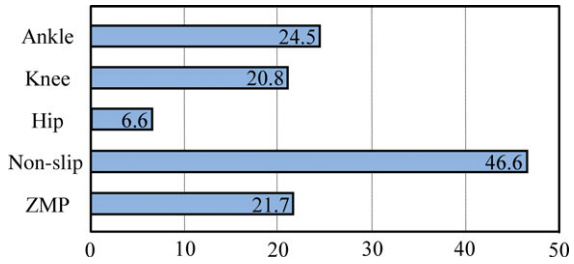

Fig. 17. (Colour online) Intervals of constraint saturation during one step.

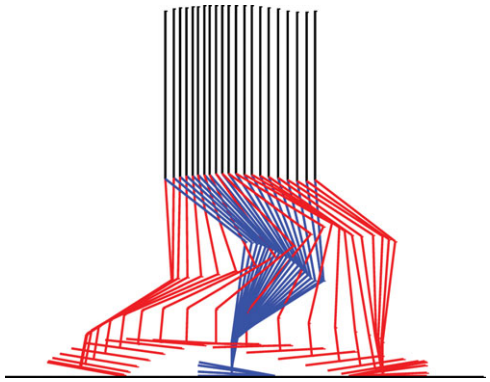

Fig. 18. (Colour online) Stick diagram of biped motion during a step.

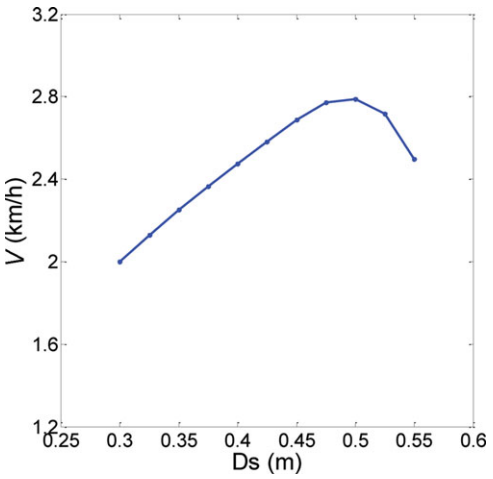

Fig. 19. (Colour online) Variation of walking speed vs. step length.

backward integrations necessary for this solution, which is performed by ODE45 function of MATLAB 2011 with step size 0.001 on a core (TM) i5–2430 M CPU@ 2.4 GHz personal computer.

So far, the minimum time necessary to take one step was calculated. It is believed that the overall speed of biped is increased with choosing larger D_s. To see the effect of D_s on the overall speed, 11 values were chosen for D_s within physically possible bounds of 0.3 m to 0.55 m and the minimum motion time was solved for each value of D_s. The study revealed that for this biped the maximum overall speed of 2.79km/h is achieved at $D_s = 0.50$m and increasing D_s beyond this value has an undesirable effect on increasing the speed. The variation of walking speed in terms of step length is shown in Fig. 19.

https://doi.org/10.1017/S0263574713000039 Published online by Cambridge University Press

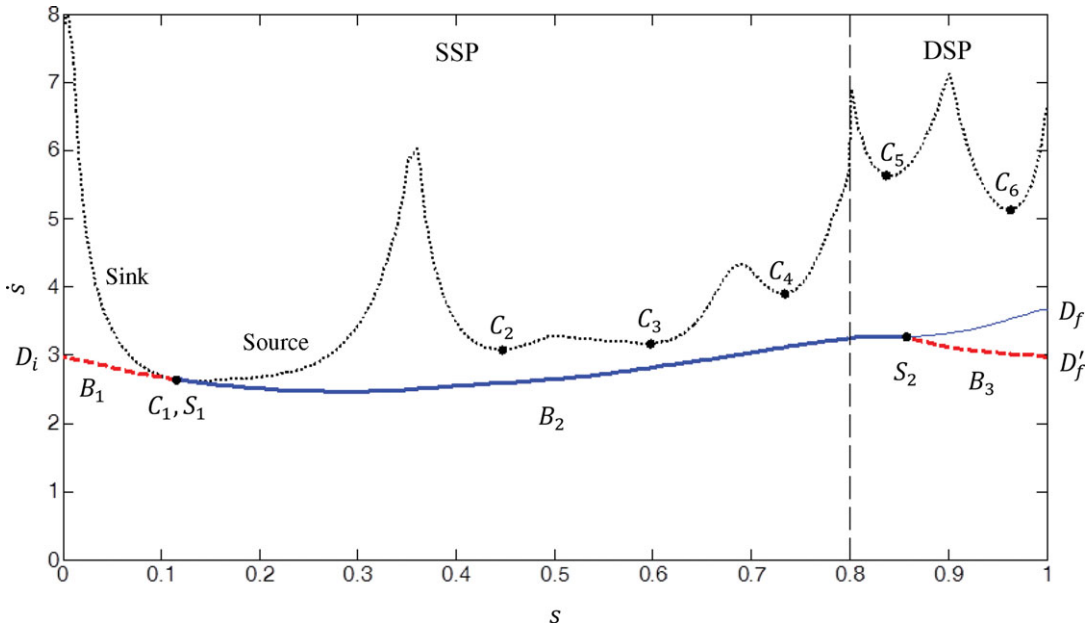

Fig. 20. (Colour online) Schematic diagram of the NFB and solution curve.

Table III. The physical parameters of the biped robot.

Links	Feet	Shin	Thigh	Trunk
Length (m)	0.21	0.3	0.3	0.7
Mass (kg)	2.3	2	1.7	44
Inertia (kg.m^2)	0.01	0.025	0.022	2.53
Mass center position (m)	0.05	0.15	0.17	0.31
Feet characteristics		l_h	l_f	l_a
		0.09 m	0.12 m	0.1 m
Motors		Ankle	Knee	Hip
Torque max (N.m)		130	170	150

5.2. Example 2

The purpose of this example is to compare the results of the proposed method with those reported by Tlalolini *et al.*[20] for minimum time motion. They solved a multi-objective optimization problem to find a path that gives the best energy-efficient stable motion of a biped while moving with a desired speed. They tried to find the maximum speed of biped through a parameter study approach where the maximum speed is found by increasing the desired speed step by step. The physical parameters of this biped are given in Table III. The maximum speed reported by Tlalolini *et al.*,[20] which is obtained for a friction coefficient of $\mu = 2/3$, is $V_{\max} = 4.8$km/h. Solving the same problem with the method presented in this paper gives the maximum achievable speed of $V_{\max} = 6$km/h showing an almost 25% improvement in the maximum speed. This result is obtained for $D_s = 0.60$m and $s_c = 0.80$ and for the other kinematic parameters as given in Table I. Figure 20 shows the minimum time path of this problem that starts at $D_i(0, 2.98)$ with $\ddot{s}_{\min}$, which is switched at points $S_1(0.115, 2.649)$ and $S_2(0.857, 3.276)$ and ends at $D'_f(1, 2.98)$.

6. Conclusion

A phase-plane analysis was presented for the minimum time path planning for a biped during one step that consists of SSP and DSP. The motion is planned to satisfy both kinematic constraints of motion such as avoiding impact with the ground and dynamic constraints such as the non-slipping condition and joint torque limits together with the stability criteria. To this end, all geometric, dynamics, and stability and non-slip constraints are expressed in terms of non-dimensional horizontal position of hip joint, s. The problem was then casted in a form similar to the problem of minimum time motion of a manipulator moving on a specified path and solved through a phase-plane algorithm. Solution is given for both SSP and DSP, which needs solution algorithms for serial and parallel manipulators. An algorithm was proposed to enforce periodicity condition at the beginning and end of each step. Numerical examples are given to clarify and validate the proposed method. Although the proposed algorithm was successful in planning minimum time motion on a specified gait, it cannot be used to perform gait optimization. This should be considered as a further extension of the present work.

Appendix: Construction of the non-feasible boundary

As explained in Section 4, construction of NFB in phase plane based on a search algorithm for points at which $\ddot{s}_{\min} = \ddot{s}_{\max}$ is tedious and numerically expensive was done. Recalling constraint equations of the problem (3), they may be written for $s = s_d$ as follows:

$$\begin{cases} \bar{\mathbf{c}}(s_d)\ddot{s} + \bar{\mathbf{d}}(s_d)\dot{s}^2 + \bar{\mathbf{e}}(s_d) = \mathbf{\Lambda} & \text{(SSP)} \\ \mathbf{c}(s_d)\ddot{s} + \mathbf{d}(s_d)\dot{s}^2 + \mathbf{e}(s_d) = \bar{\mathbf{A}}(s_d)\mathbf{\Lambda} & \text{(DSP)} \end{cases},$$
$$\mathbf{\Lambda}_{\min} \le \mathbf{\Lambda} \le \mathbf{\Lambda}_{\max}. \qquad (39)$$

These equations are linear in terms of $\ddot{s}$ and $\dot{s}^2$ for any specific value of s_d. It is clear that the values of $\ddot{s}_{\max}$, $\ddot{s}_{\min}$, and $\dot{s}^2_{\max}$ occur on the boundary of a polygon in $\ddot{s} - \dot{s}^2$ plane.

https://doi.org/10.1017/S0263574713000039 Published online by Cambridge University Press

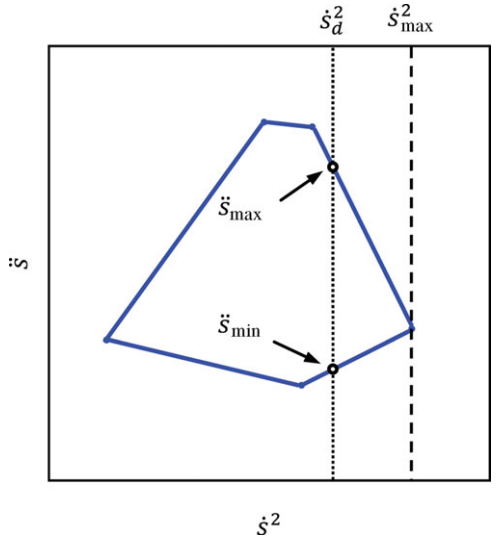

Fig. 21. (Colour online) Typical polygon for certain value of s.

Inspection of these equations reveals that the form of equations during SSP is similar to those of a serial manipulator. On the other hand, the form of equations during DSP is similar to those of a parallel manipulator, for which the matrix $\bar{\mathbf{A}}$ is not square. What follows introduces a direct method that can be used to construct NFB during both SSP and DSP.

Single support phase

Pfeiffer and Johanni[23] stated that for a n DOF serial manipulator, equations of motion can be written as n independent equations in the following form:

$$\bar{c}_i \ddot{s} + \bar{d}_i \dot{s}^2 + \bar{e}_i = \Lambda_i \quad i = 1, \ldots, n,$$
$$\Lambda_{\min_i} \leq \Lambda_i \leq \Lambda_{\max_i}. \tag{40}$$

The solution to each of these n equations is an area between two parallel straight lines in $\ddot{s} - \dot{s}^2$ plane. Intersection of these areas shows a polygon whose interior area gives the admissible values for $\ddot{s}$ and $\dot{s}$ for s_d (see Fig. 21). It can be seen from Fig. 21 that for each value of s_d, $\dot{s}_d$ there exists a range of admissible $\ddot{s}$ while there exists one $\dot{s}_{\max}$ for each value of s_d, corresponding to the point on NFB. This method could be used for any $s_d \leq s_c$, i.e., in SSP to construct NFB.

Double support phase

It seems that the same solution as presented by Pfeiffer and Johanni[23] holds for parallel manipulator except that the $2n$ parallel lines must be obtained using the maximum and minimum of $\bar{\mathbf{\Lambda}} = \bar{\mathbf{A}}\mathbf{\Lambda}$. Sadigh *et al.*[32] showed that, due to coupling of equations with respect to $\mathbf{\Lambda}$, the admissible area in $\ddot{s} - \dot{s}^2$ plane is not equal to the interior area of the polygon constructed from the $2n$ lines corresponding to the n equations of motion.

Considering $\bar{\mathbf{A}}$ is a $n \times m$ matrix where $n < m$, McCarthy and Bobrow[33] showed that for any feasible solution at least $m - n + 1$ actuators could be saturated. Considering this fact, one might rewrite Eq. (39) during DSP in the following partitioned form:

$$\mathbf{c}\,\ddot{s} + \mathbf{d}\,\dot{s}^2 + \mathbf{e} = [\bar{\mathbf{A}}_{a_{n\times n}} \quad \bar{\mathbf{A}}_{b_{n\times(m-n)}}] \begin{bmatrix} \mathbf{\Lambda}_{a_{n\times 1}} \\ \mathbf{\Lambda}_{b_{(m-n)\times 1}} \end{bmatrix}, \tag{41}$$

and pre-multiplying Eq. (41) with $\bar{\mathbf{A}}_a^{-1}$ results:

$$\tilde{\mathbf{c}}\,\ddot{s} + \tilde{\mathbf{d}}\,\dot{s}^2 + \tilde{\mathbf{e}} = \mathbf{\Lambda}_{a_{n\times 1}}, \tag{42}$$

where

$$\tilde{\mathbf{c}} = \bar{\mathbf{A}}_a^{-1}\mathbf{c},\ \tilde{\mathbf{d}} = \bar{\mathbf{A}}_a^{-1}\mathbf{d},\ \tilde{\mathbf{e}} = \bar{\mathbf{A}}_a^{-1}(\mathbf{e} - \bar{\mathbf{A}}_b\mathbf{\Lambda}_b).$$

This relation means that at each point $(s_d, \dot{s}_d)$ $m - n$ additional $\mathbf{\Lambda}$ selected as $\mathbf{\Lambda}_b$ may adopt its saturation value compared to the case of a serial manipulator, e.g., at least $m - n + 1$ out of m quantities of Λ_i are saturated on the solution trajectory.[33]

Equation (42) is now of the same format as Eq. (40) of a serial manipulator, whose solution is the interior area of a polygon constructed from n couples of parallel straight lines. As we have $C(m, m-n)$ choices for $\mathbf{\Lambda}_b$, i.e., different choices of saturated quantities of $\mathbf{\Lambda}$, there would be $C(m, m-n)$ polygons that the interior area of their intersection shows the area of admissible $\ddot{s}$, $\dot{s}$ for the certain value s_d. Although construction of such a polygon is rather time consuming, it does not need any search algorithm to find $\dot{s}_{\max}$ and it is still much more numerically efficient as compared to the search algorithm described in Section 4.

References

1. M. Vukobratovic and J. Stepanenko, "On the stability of anthropomorphic systems," *Math. Biosci.* **15**, 1–37 (1972).
2. M. Vukobratovic and B. Borovac, "Zero-moment point: Thirty-five years of its life," *Int. J. Humanoid Robot.* **1**(1), 157–173 (2004).
3. S. Kajita and K. Tani, "Study of Dynamic Biped Locomotion on Rugged Terrain: Derivation and Application of the Linear Inverted Pendulum Mode," *Proceedings of the IEEE ICRA*, Sacramento, CA (Apr. 9–11, 1991) pp. 1405–1411.
4. S. Kajita, F. Kanehiro, K. Kaneko, K. Yokoi and H. Hirukawa, "The 3D Linear Inverted Pendulum Mode: A Simple Modeling for a Biped Walking Pattern Generation," *Proceedings of the IEEE/RSJ International Conference on Intelligent Robots and Systems*, Maui, HI (Oct. 29–Nov. 3, 2001) pp. 239–246.
5. J. H. Park and K. D Kim, "Biped Robot Walking Using Gravity-Compensated Inverted Pendulum Mode and Computed Torque Control," *Proceedings of IEEE ICRA*, Leuven, Belgium (May 16–20, 1998) pp. 3528–3533.
6. K. Erbatur and O. Kurt, "Natural ZMP trajectories for biped robot reference generation," *IEEE Trans. Ind. Electron.* **56**(3), 835–845 (2009).
7. A. Takanishi, M. Tochizawa, H. Karkai and I. Kato, "Dynamic Biped Walking Stabilized with Optimal Trunk and Waist Motion," *Proceedings of IEEE/RSJ International Workshop on Intelligent Robots and Systems*, Tsukuba, Japan (Sep. 4–6, 1989) pp. 187–192.
8. J. I. Yamaguchi, A. Takanishi and I. Kato, "Development of Biped Walking Robot Compensating for Three-Axis Moment by Trunk Motion," *Proceedings of IEEE/RSJ International Conference on Intelligent Robots and Systems*, Yokohama, Japan (Jul. 26–30, 1993) pp. 561–566.
9. Q. Huang, K. Yokoi, S. Kajita, K. Kaneko, H. Arai, N. Koyachi and K. Tanie, "Planning walking patterns for a biped robot," *IEEE Trans. Robot. Autom.* **17**(3), 280–289 (2001).

https://doi.org/10.1017/S0263574713000039 Published online by Cambridge University Press

10. P. H. Channon, S. H. Hopkins and D. T. Pham, "Derivation of optimal walking motions for a bipedal walking robot," *Robotica* **10**, 165–172 (1992).
11. J. H. Park and M. S. Choi, "Generation of an optimal gait trajectory for biped robots using a genetic algorithm," *JSME Int. J. Series C* **47**(2), 715–721 (2004).
12. V. H. Dau, C. M. Chew and A. N. Poo, "Achieving energy-efficient bipedal walking trajectory through GA-based optimization of key parameters," *Int. J. Humanoid Robot.* **6**(4), 609–629 (2009).
13. M. Rostami and G. Bessonet, "Sagittal gait of a biped robot during the single support phase. Part 2: Optimal motion," *Robotica* **19**, 241–253 (2001).
14. G. Capi, Y. Nasu, L. Barolli, K. Mitobe and K. Takeda, "Application of genetic algorithms for biped gait synthesis optimization during walking and going up-stairs," *Adv. Robot.* **15**(6), 675–694 (2001).
15. T. Saidouni and G. Bessonnet, "Generating globally optimised sagittal gait cycles of a biped robot," *Robotica* **21**, 199–210 (2003).
16. G. Bessonnet, S. Chesse and P. Sardain, "Optimal gait synthesis of a seven-link planar biped," *Int. J. Robot. Res.* **23**(10–11), 1059–1073 (2004).
17. C. Chevallereau and Y. Aoustin, "Optimal reference trajectories for walking and running of a biped robot," *Robotica* **19**, 557–569 (2001).
18. S. Miossec and Y. Aoustin, "A simplified stability study for a biped walk with underactuated and overactuated phases," *J. Robot. Res.* **24**(7), 537–551 (2005).
19. G. Dip, V. Prahlad and P. D. Kien, "Genetic algorithm-based optimal bipedal walking gait synthesis considering tradeoff between stability margin and speed," *Robotica* **27**, 355–365 (2009).
20. D. Tlalolini, C. Chevallereau and Y. Aoustin, "Comparison of different gaits with rotation of the feet for a planar biped," *J. Robot. Auton. Syst.* **57**(4), 371–383 (2009).
21. M. J. Sadigh and S. Mansouri, "Effect of Step Size and Step Period on Feasible Motion of a Biped Robot," *Proceedings of IEEE International Conference on Robotics and Biomimetics (ROBIO)*, Tianjin, P. R. China (Dec. 14–18, 2010) pp. 1–6.
22. J. E. Bobrow, S. Dubowsky and J. S. Gibson, "Time-optimal control of robotic manipulators along specified paths," *Int. J. Robot. Res.* **4**(3), 3–17 (1985).
23. F. Pfeiffer and R. Johanni, "A concept for manipulator trajectory planning," *IEEE Trans. Robot. Autom.* **3**(2), 115–123 (1987).
24. L. Zlajpah, "On Time Optimal Path Control of Manipulators with Bounded Joint Velocities and Torques," *Proceedings of IEEE ICRA*, Minneapolis, MN (1996) pp. 1572–1577.
25. M. H. Ghasemi and M. J. Sadigh, "A direct algorithm to compute the switching curve for time-optimal motion of cooperative multi-manipulators moving on a specified path," *Adv. Robot.* **22**, 493–506 (2008).
26. D. Verscheure, B. Demeulenaere, J. Swevers, J. De Schutter and M. Diehl, "Time-optimal path tracking for robots: A convex optimization approach," *IEEE Trans. Autom. Control* **54**(10), 2318–2327 (2009).
27. S. B. Moon and S. Ahmad, "Time optimal trajectories for cooperative multi-robot systems," *Proc. IEEE Int. Conf. Decision Control* **2**, 1126–1127 (1990).
28. S. B. Moon and S. Ahmad, "Time scaling of cooperative multi robot trajectory," *IEEE Trans. Syst. Man Cybern.* **21**(4), 900–908 (1991).
29. J. E. Bobrow, J. M. McCarthy and V. K. Chu, "Minimum-time trajectories for two robots holding the same workpiece," *Proc. IEEE Int. Conf. Decision Control* **6**, 3102–3107 (1990).
30. M. J. Sadigh and M. H. Ghasemi, "A Fast Algorithm Time Optimal Control of a Cooperative Multi Manipulator System on Specified Path," *Proceedings of 5th Vienna Conference on Mathematical Modeling (MATHMOD)*, Vienna, Austria (Feb. 8–10, 2006) pp. 1–7.
31. M. H. Ghasemi, Coordinated Minimum Time Motion of a Cooperative Multi Manipulator System Along a Specified Path, *PhD Dissertation* (Isfahan: Department of Mechanical Engineering, Isfahan University of Technology, 2008, in Persian).
32. M. J. Sadigh, M. H. Ghasemi and M. Keshmiri, "A Direct Algorithm to Compute Switching Curve for Time Optimal Motion of Cooperative Multi-Manipulators Moving on Specified Path," *Proceedings of 13th IEEE IFAC International Conference on Methods and Models in Automation and Robotics (MMAR)*, Szczecin, Poland (Aug. 27–30, 2007) pp. 875–882.
33. J. M. McCarthy and J. E. Bobrow, "The number of saturated actuators and constraint forces during time-optimal movement of a general robotic system," *IEEE Trans. Robot. Autom.* **8**(3), 407–409 (1992).

https://doi.org/10.1017/S0263574713000039 Published online by Cambridge University Press